19th Brazilian Congress of Thermal Sciences and Engineering
November 06th-10th, 2022, Bento Gonçalves - RS - Brazil

ENC-2022-0238
THERMODYNAMIC ANALYSIS OF THE INFLUENCE OF CARBON DIOXIDE AS DILUENT IN OXY-FUEL COMBUSTION GAS TURBINES

Rafael Pinho Furtado
Antonio Garrido Gallego
Federal University of ABC, Santo André, São Paulo, Brazil
rafael.furtado@aluno.ufabc.edu.br, a.gallego@ufabc.edu.br

Silvia Azucena Nebra
Federal University of ABC, Santo André, São Paulo, Brazil
silvia.nebra@ufabc.edu.br

André Vilela
Federal University of ABC, Santo André, São Paulo, Brazil
agcvilela@outlook.com

Reynaldo Palacios-Bereche
Federal University of ABC, Santo André, São Paulo, Brazil
reynaldo.palacios@ufabc.edu.br

Abstract. *Oxy-fuel combustion is an important technology to reduce carbon dioxide emissions in thermal power plants like boilers and gas turbines. The use of oxy-fuel in gas turbines implies substituting air for oxygen with carbon dioxide or water in the dilution process in the combustion process. The substitution of carbon dioxide and water as working fluid, that is, the carbon dioxide would replace the air, the usual working fluid. The gas properties of this working fluid differ significantly from those of a conventional air-breathing gas turbine; hence, the gas turbine must be designed accordingly. The combustion with nearly pure oxygen can reach temperatures around 2500 °C, much higher than the thermal capacity of the materials employed in combustors and turbines. Then, to control the combustion chamber temperature, the oxygen is diluted with a portion of flue gas. The flue gas produced is composed mainly of carbon dioxide and water vapour. They were making it possible to separate the water from the flue gas by condensation and avoiding more complex separation processes, such as chemical absorbents, which is the main advantage of oxy-fuel technology. On the other hand, the nearly pure oxygen stream, containing about 90-99.5 mol%, is produced in an air separation unit, which has a high energy consumption and penalizes the power plant efficiency. In this work, two oxy-fuel gas cycles were analyzed among those present in the literature: the semi-closed oxy-fuel combined cycle (SCOC-CC) and the E-Matiant. The main objective of the analysis is to identify the advantages and disadvantages of these cycles utilizing the first and second laws of thermodynamics and the theory of exergy cost, thereby helping to determine the influence of using CO_2 as diluent in oxy-fuel combustion and the sources of the cycle's thermodynamic inefficiencies. The energy efficiency of the SCOC-CC and E-Matiant are, respectively, 49.14% and 47.65%. The exergy efficiency is 46.94% for the SCOC-CC and 53.79% for the E-Matiant. In comparison to a conventional combined cycle, these cycles are less efficient, but they have the great advantage of capturing all the carbon dioxide produced in the combustion, which makes them attractive from an environmental perspective.*
Keywords: *Oxy-fuel; E-Matiant, SCOC-CC, CO_2 Capture, Exergy cost*

1. INTRODUCTION

In order to contain global warming, the Paris agreement was proposed in 2015 at the United Nations Conference on Climate Change (COP21), whose main objective is to limit the increase in the global average temperature to 2°C, preferably 1.5°C, compared to the pre-industrial period (United Nations, 2022). Thus, it will be necessary to reduce the greenhouse gas emissions by 7.6% per year between 2020-2030 to reach the 1.5°C limits, and a reduction by 2.7% per year for the 2 °C limits, in order to achieve the Paris agreement objective (United Nations, 2022).Several alternatives can be used to reduce CO_2 emissions: improvements in energy efficiency, utilization of low carbon fuels, increasing the use of sources with low or near-zero CO_2 emissions, development and usage of Carbon Capture and Storage technologies

(CCS), changes in land use and management (EPA, 2022). According to Dahlquist (2016), carbon capture and storage technologies is a generic term that involves technologies where CO_2, formed through oxidation (combustion) of fossil fuels, is captured at some stage of a process. CCS technologies are applicable in power generation, plants that burn fossil fuels, and industrial processes such as cement and steel production. CCS technologies are divided into three groups: oxy-fuel combustion, pre-combustion, and post-combustion; however, according to Nascimento (2018), there is still no consensus in the literature on which of the technologies is the best.

In the oxy-fuel, combustion takes place in the presence of a stream containing about 90-99,5 mol% oxygen. Thus, the combustion products are a stream composed mainly of water, CO_2, and other impurities present in the oxygen stream and fuel. One of the advantages of oxy-combustion is that water can be removed easily from combustion products by condensation. On the other hand, an air separation unit is required to produce oxygen, this unit has high energy consumption. The combustion of a fuel with almost pure oxygen has a combustion temperature of about 2500°C, which is too high for conventional power plant materials. The combustion temperature is limited to approximately 1300-1400°C in a typical gas turbine cycle and about 1900°C in a coal-fired boiler using the current technology; thus, part of the flue gases is recycled to the combustor to control the combustion temperature (Metz et al., 2005). Oxy-fuel combustion gas cycles are an alternative to CO_2 capture in gas-fired power plants, and several authors have proposed different oxy-fuel combustion gas cycles. This work performs an analysis of two oxy-fuel cycles to identify their advantages, disadvantages and potential use. Among the oxy-fuel combustion gas cycles available in the literature, the following two were chosen for analysis: semi-closed oxy-fuel combustion combined cycle (SCOC-CC) and E-Matiant. The cycles analysis takes into account energy, exergy and exergy cost balances, thereby helping to determine the influence of using CO_2 as diluent in oxy-fuel combustion and to identify the sources of the cycle's thermodynamic inefficiencies at the component level.

1.1 Semi-closed oxy-fuel combined cycle (SCOC-CC)

The semi-closed oxy-fuel (SCOC-CC) is similar to a conventional combined cycle, except that the fuel is burned using nearly pure oxygen. The Brayton cycle of SCOC-CC utilizes CO_2 recycled from the flue gases as working fluid and works at higher pressure ratios than conventional Brayton cycles (approximately 40) due to the low specific heat of CO_2 (Sundkvist et al., 2014). Exhaust gases (mainly composed of H_2O and CO_2) from the Brayton cycle provide heat to a Rankine cycle via a heat recovery steam generator (HRSG). After leaving the HRSG, the exhaust gases are cooled to condense the water and separate it from the CO_2. Approximately 90% of the CO_2 is recycled in the gas turbine compressor (Kvamsdal et al., 2007). According to IEAGHG (2015), the SCOC-CC is the simplest oxy-fuel gas cycle proposed in the literature. However, its implementation requires the development of new compressors and turbines for the Brayton cycle. The CO_2 gas turbine requires a redesign to optimize the blade geometry and the cooling channels due to the CO_2-rich working fluid. There are no fundamental technical barriers to developing CO_2 gas turbines, as they can be designed with the same criteria used by conventional gas turbine manufacturers.

The SCOC-CC is presented in Figure 1. In this cycle, CO_2 (stream 1) is compressed until the combustion chamber pressure (stream 2). Then this CO_2 stream, fuel (stream 5) and oxygen provided by the ASU (stream 8) are fed into the combustion chamber. The combustion products (stream 3) are expanded in the GT turbine (stream 4), and the flue gases provide heat for a steam cycle (stream 16 to 22) via a dual pressure HRSG. The water in the flue gases (stream 11) is then removed in the dehumidifier. Then the CO_2 (stream 13) is divided into two streams, about 90% of stream 13 mass flow is recycled to the gas turbine compressor (stream 1), and the other part (stream 14) is compressed until 100 bar and captured (stream 15). The energy efficiency of this cycle is expected to be between 45-48% (IEAGHG, 2015).

1.2 E-Matiant

The E-Matiant cycle, Fig. 2, is similar to an Ericcson cycle. It is composed of multi-stage CO_2 compression with intermediate cooling, one or more combustors followed by adiabatic expansions in CO_2 turbines and a recuperator. Figure 2 shows the E-Matiant cycle and its temperature-entropy (T-s) diagram. In this cycle, CO_2 (stream 7) is compressed in a 4-stage intercooled compressor until the combustion chamber pressure (stream 8). Then stream 8 is divided into two streams (streams 9 and 15). Stream 15 is the CO_2 excess that is compressed until 100 bar and captured. The other part of stream 8 (stream 9) is pre-heated in a recuperator before it enters the combustion chamber (stream 1). The combustion chamber is fed with CO_2 (stream 1), oxygen provided by the ASU (stream 2) and fuel (stream 3), and the combustion products (stream 4) are CO_2, H_2O and impurities from the fuel and oxygen. The combustions products at high temperature and pressure are expanded in a CO_2 turbine (stream 5), and then the expanded gases are cooled in the recuperator (process 5-6). The water present in the combustion product is removed (stream 15) in a dehumidifier, while CO_2 is recirculated in the cycle (stream 7).

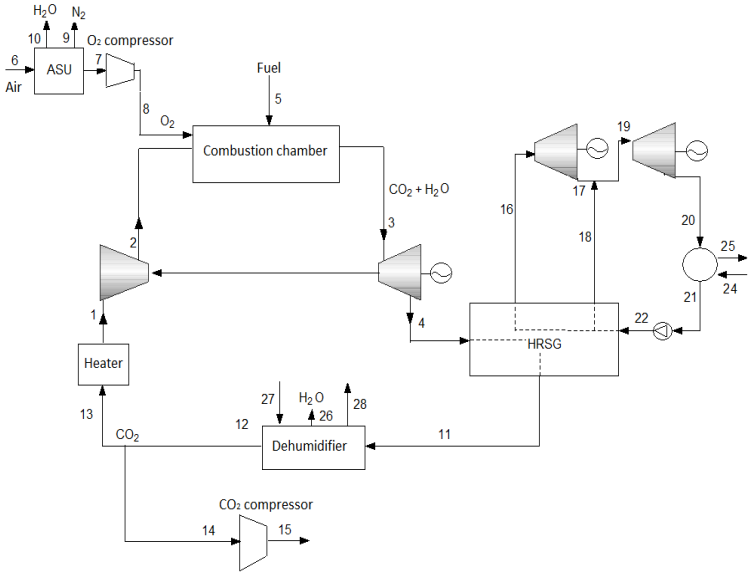

Figure 1. Semi-closed oxy-fuel combined cycle.

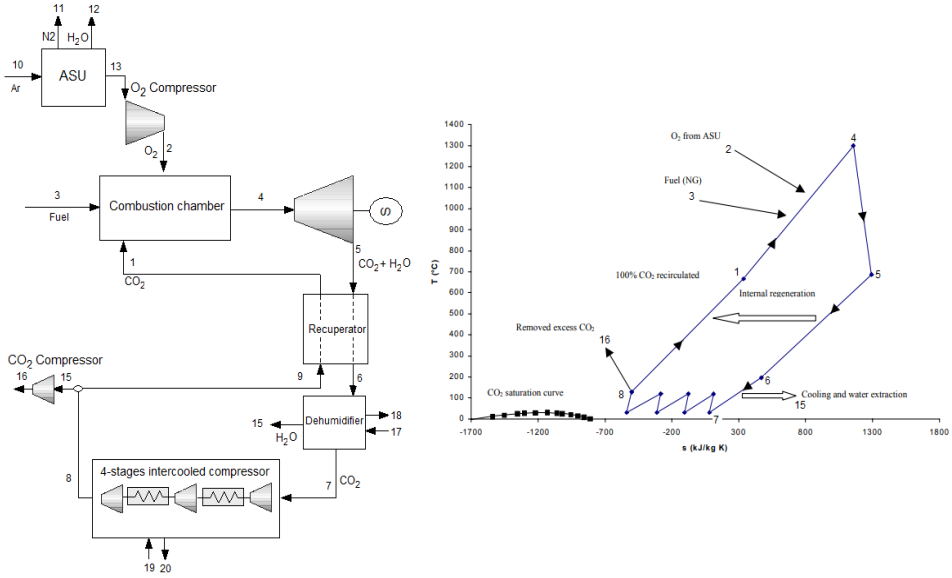

Figure 2. E-Matiant cycle (Adapted from IEAGHG, 2015).

2. METHODOLOGY

This article proposed to carry out an analysis of the SCOC-CC and E-Matiant cycle, considering energy, exergy and exergy cost. The computational models of the cycles were developed in Engineering Equation Solver (EES). Following the development of the models, those were validated utilizing the same thermodynamic assumption from the models developed by Kvamsdal et al. (2007) for the SCOC-CC and Mathieu (2000) for the E-Matiant cycle. The energy efficiency obtained by the authors were compared with the energy efficiency obtained by the computational model developed in EES. After the validation, optimization problems were proposed to find the maximal energy efficiency for the given temperature, pressure and oxygen purity limits that will be presented later. From the optimal point found for both cycles, a thermodynamic analysis of the cycles was done considering a fixed fuel consumption of 1 kg/s.

2.1 Thermodynamic analysis

The thermodynamic analysis was performed through mass balance, Eq. (1); energy balance, Eq. (2); exergy balance, Eq. (3); and exergy cost balance, Eq. (4). A control volume enclosing each component is at steady-state, and potential/kinetic energy effects are negligible. The ambient pressure is 1.013bar, and the ambient pressure is 25°C.

$$\left(\sum \dot{m}_i\right)_{out} = \left(\sum \dot{m}_i\right)_{in} \quad (1)$$

$$0 = \dot{Q} - \dot{W} + \left(\sum \dot{m}_i h_i\right)_{in} - \left(\sum \dot{m}_i h_i\right)_{out} \quad (2)$$

$$0 = \sum \left(1 - \frac{T_0}{T}\right) \dot{Q} - \dot{W} - \left(\sum \dot{m}_i ex_i\right)_{in} - \left(\sum \dot{m}_i ex_i\right)_{out} - \dot{I} \quad (3)$$

$$\left(\sum Ex_i k_i\right)_{out} = \left(\sum Ex_i k_i\right)_{in} \quad (4)$$

Where $\dot{m}$ is the mass flow rate (kg/s); i is the state point or index i; $\dot{Q}$ is thermal energy rate (kW); $\dot{W}$ is power (kW); h is the specific enthalpy (kJ/kg); T_0 reference temperature (298K); T is temperature (K); ex is specific exergy (kJ/kg); $\dot{I}$ is the exergy destruction rate of irreversibility (kW); Ex is the exergy flow (kW); k is the unitary exergy cost.

The specific exergy of all flows (except fuel) is given by Eq. (5). The chemical exergy of the fuel is given by Eq. (6). The performance of each cycle is evaluated using energy efficiency Eq. (7) and exergy efficiency Eq. (8).

$$ex = (h - h_0) - T_0(s - s_0) \quad (5)$$

$$ex_{fuel} = \sum \left(y_i ex_{ch,i,0} + R_i T_0 (y_i \ln y_i)\right) / M \quad (6)$$

$$\eta_I = \frac{W_{net}}{m_{fuel} LHV} \quad (7)$$

$$\eta_{II} = 1 - \frac{I_{tot}}{m_{fuel} ex_{fuel}} \quad (8)$$

Where ex is the specific exergy (kJ/kg); ex_{fuel} is the fuel exergy (kJ/kg); h_0 is enthalpy in reference condition (kJ/kg); s_0 is entropy in reference condition (kJ/kg-K); s is entropy (kJ/kg-K); y_i is the molar fraction of of each component i; $ex_{ch,i,0}$ is standard chemical exergy (kJ/kg); R_i is the gas constant of each component i; W_{net} is the net power of the cycle (kW); m_{fuel} is the fuel mass flow (kg/s); M is the molar mass (kg/kmol), LHV is the lower heating value of fuel (kJ/kg), I_{tot} is the total plant irreversibility (kW).

Turbines, pumps, and compressors were assumed to be adiabatic. The gas turbine compressor, expander and 4-stages intercooled compressor have a polytropic efficiency of 91%. The high-pressure steam turbines isentropic efficiency is 92%, and the low-pressure steam turbines isentropic efficiency is 89% (Kvamsdal et al., 2007). The captured CO_2 compression is done in 4 stages with intermediate cooling to reduce the compressors energy consumption. The three initial stages compress the CO_2 to its critical pressure (about 72bar); the last stage is done in a pump until 100 bar. It was considered the isentropic efficiency 85%, 80%, 75% and 75% in the first, the second and the third and fourth stages, respectively. (Kvamsdal et al., 2007). The O_2 compressions are done in 3 stages with intermediate cooling and the same isentropic efficiencies as the CO_2 compression was assumed. The efficiency of generators is 98.5% (Sheldrake, 2016).

The combustion processes are assumed stoichiometric, and the pressure drop of 5% was considered in the combustion chamber. The fuel composition is presented in Tab. 1, and the fuel lower heating value is 46480 kJ/kg.

The HRSG of the SOCC-CC has two pressure levels, consisting of three heat exchangers (economizer, evaporator and superheat) for each pressure level. It was considered that the high-pressure level water is pre-heated in the low-pressure economizer and then it is pumped to the high-pressure economizer. A pressure loss of 40 mbar was assumed on the flue gases side of the HRSG (Kvamsdal et al., 2007); on the water/steam side, pressure losses were neglected. For HRSG design, the pinch point is between 8-20 °C, and the approach point is between 5-12 °C (Bolland, 2010) (Kehlhofer, 2009). For the HRSG design, it was considered an approach point of 12° C for low and high-pressure economizers, the pinch point of the low-pressure evaporator is 15° C, and the high-pressure evaporator pinch point is 20°C. In addition to the pinch and approach point, a temperature difference of 35° C was considered between the high-pressure steam turbine inlet temperature and the gas turbine exhaust gases on the HRSG inlet. Table 2 presents the usual nominal temperature and pressure ranges for the HRSG (Bojici and Neaga, 2012). A pressure drop of 2% was assumed on the hot and cold sides of the E-Matiant recuperator.

Table 1. Fuel composition (Bolland, 2010).

CH_4	C_2H_6	C_3H_8	C_4H_{10}	C_6H_{14}	CO_2	N_2
89%	7%	1%	0.1%	0.001%	2%	0.8999%

Table 2. HRSG usual nominal pressure and temperature ranges (Bojici and Neaga, 2012).

High-pressure level		Low-pressure level	
Temperature (°C)	500-565	Temperature (°C)	200-260
Pressure (bar)	55-85	Pressure (bar)	3-8

An air separation unit by cryogenic distillation was chosen for oxygen production since cryogenic distillation is the most mature and reliable technologies, as it has been in practice for over 75 years (NETL, 2022). The purity of the oxygen produced by the ASU is an important parameter for oxy-fuel combustion power plants as purer oxygen streams increase ASU energy consumption, decreasing power plant efficiency. On the other hand, an oxygen stream with low oxygen purity will produce flue gases with more impurities, increasing the cost and energy consumption of the CO_2 treatment and compression unit (Zheng, 2011). The specific energy consumption of ASU by cryogenic distillation as a function of oxygen purity was parameterized by Hu et al. (2010). The specific energy consumption is given by Eq. (9) if the oxygen purity is equal to or lower than 97mol% and by Eq. (10) if the oxygen purity is greater than 97mol%. The molar composition of the oxygen stream supplied by the ASU is shown in Tab. 3 for different values of oxygen purity. It was assumed that atmospheric air enters the ASU at ambient temperature and pressure (25 °C, 1,013 bar) and 60% relative humidity, all the water is condensed before the cryogenic distillation process and leaves the unit at 29.5 °C and 3.1 bar, the N_2 stream leaves the unit at 27 °C and 1.013 bar, while the oxygen stream leaves the unit at 0.1 °C and 4.7 bar (Ebrahimi et al., 2015).

$$e_{ASU}=92.3103 + 8.2457\, y_{O_2} \tag{9}$$

$$e_{ASU}=383.3773/(100 - y_{O_2})^{0.4577} + 660.0583 \tag{10}$$

Where e_{ASU} is ASU specific energy consumption (kJ/kg); y_{O_2} is oxygen purity (mol%).

Table 3. Oxygen stream molar composition (Hu et al., 2010).

O_2	0.910	0.920	0.930	0.940	0.950	0.960	0.970	0.980	0.990
Ar	0.039	0.040	0.040	0.041	0.041	0.040	0.030	0.020	0.010
N_2	0.051	0.040	0.030	0.019	0.009	0	0	0	0

The supplementary equations utilized for the exergy cost balance are presented in Tab. 4. These equations are proposed according to the "Theory of the Exergetic Cost" presented by Lozano and Valero (1993). The indexes are numbered accordingly to Fig. 1 for the SCOC-CC and Fig. 2 for the E-Matiant.

Table 4. Supplementary equations for exergy cost analysis.

SCOC-CC		E-Matiant	
$k_5= k_6= k_{24}= k_{27}=1$	$k_{16}= k_{17}$	$k_3= k_{10}= k_{17}= k_{19}=1$	$k_{turbine}= k_{4\text{-stages-compr}}$
$k_9= k_{10}= k_{24}= k_{26}= k_{28}=0$	$k_{16}= k_{18}$	$k_{11}= k_{12}= k_{14}= k_{18}= k_{20}=0$	$k_{power\ consumed}= k_{elect\ power}$
$k_3= k_4$	$k_{17}= k_{19}$	$k_4= k_5$	
$k_4= k_{11}$	$k_{19}= k_{20}$	$k_5= k_6$	
$k_{12}= k_{13}$	$k_{GTturbine}= k_{Gtcomp}$	$k_9= k_8$	
$k_{12}= k_{14}$	$k_{power\ consumed}= k_{elect\ power}$	$k_{15}= k_8$	

2.2 Energy efficiency optimization

The energy efficiency optimization problems were defined according to the temperature and pressure at the turbine's inlet, the purity of the oxygen stream produced by the ASU, the condensing pressure of the Rankine cycles, and the temperature of the flue gases at the outlet of the dehumidifier. The problems were formulated respecting the operational limitations of each device. The pressure ratio of CO_2 gas turbines is in the range of 30-40 (Dahlquist, 2016). The inlet temperature of the gas turbine expander can reach temperatures next to 1500°C (Gülen, 2019), however, in this work, more modest temperatures were considered, and this temperature should be between 1000-1350°C. The temperature and pressure ate the inlet of high and low-pressure steam turbines should respect the operational range of the HRSG shown in Tab. 2. The condenser pressure of the steam cycles should be in the range of 0.74-0.88bar (GTW, 2018). It was considered that the oxygen purity should be between 90-99.5mol%, which is the appropriate range for oxy-fuel combustion plants according to (Zheng, 2011).

The energy efficiency of the SCOC-CC has been calculated as a function of gas turbine pressure ratio (pr), oxygen purity (y_{O2}), inlet temperature of gas turbine expander (TIT), the inlet pressure of low-pressure (LP) and high-pressure (HP) steam turbines, condenser pressure (CP), dehumidifier outlet temperature (DT). The inlet temperature of the high (HT) and low-pressure (LT) steam turbines are restrictions that must be respected. The energy efficiency of the E-Matiant cycle is calculated as a function of the temperature (TIT) and pressure at the inlet of the turbine, oxygen purity (y_{O2}) and temperature of flue gases at the dehumidifier outlet (DT). Table 5 shows the energy efficiency optimization problems of the SCOC-CC and E-Matiant cycle.

Table 5. Energy efficiency optimization problems.

	SCOC-CC	E-Matiant
MAXIMIZE	$\eta_I = \eta_I$(TIT, pr, y_{O2}, HP, LP, CP, DT)	$\eta_I = \eta_I$(TIT, pr, y_{O2}, DT)
Inlet temperature of gas turbine expander (TIT)	1050 - 1350 °C	1050 - 1350 °C
Gas turbine pressure ratio (pr)	30 - 40	30 – 40
Oxygen purity (y_{O2})	0.9 - 0.995 mol/mol	0.9 - 0.995 mol/mol
Inlet pressure of high-pressure steam turbine (HP)	55 - 85 bar	-
Inlet pressure of low-pressure steam turbine (LP)	3 - 8 bar	-
Condenser pressure (CP)	0.0774 - 0.088 bar	-
Dehumidifier outlet temperature (DT)	28 - 70 °C	28 - 70 °C
Inlet temperature of high-pressure steam turbine (HT)	500 - 565 °C	-
Inlet temperature of low-pressure steam turbine (LT)	200 - 260 °C	-

The optimization problems were solved by particle swarm optimization (PSO). This algorithm was implemented in MATLAB. PSO is an optimization algorithm for solving nonlinear and linear functions created by Eberhart and Kennedy (1995). It was inspired by the intelligent behaviour of groups of animals such as swarms, shoals and flocks of birds. PSO is a search technique based on the social behaviour of individuals. This behaviour initially presents a random and disordered search, but an organization in the flight is observed over time, and a search pattern is presented. When the search target is reached, all particles tend towards the objective (Silva et al., 2014).

3. RESULTS

The validation of the computational models developed in EES is presented in Tab. 6. The difference between the energy efficiency obtained by Kvamsdal et al. (2007) and the energy efficiency obtained in the EES model is 1.9% for the SCOC-CC. The difference between the energy efficiency obtained by Mathieu (2000) and the EES model is -0.7%. It is highlighted that the same thermodynamic assumptions were utilized by Kvamsdal et al. (2007) and Mathieu (2000). Considering that both authors used different softwares for developing their models, SimSci PRO/II in the case of Kvamsdal et al. (2007) and ASPEN PLUS in the case of Mathieu (2000), the results for the validation of the EES model is satisfactory.

Table 6. Computational model validation.

Energy efficiency	Kvamsdal et al. (2007)	Mathieu (2000)	EES models	Difference
SCOC-CC	47.0%	-	44.2%	1.9%
E-Matiant	-	44.5%	48.1%	-0.7%

Table 7 shows the solution obtained for the optimization problems. The optimal energy efficiency of the SCOC-CC cycle is 49.14%, and the optimal efficiency of the E-Matiant is 47.65%. At the optimal point, the temperature of the flue gases in the dehumidifier outlet (DT) was the lowest of the optimization problems for the two cycles. The turbine inlet temperature (TIT) of the E-Matiant is higher than the TIT of the SCOC-CC cycle because there are no temperature constraints for the recuperator of the E-Matiant cycle. In the SCOC-CC, the TIT is constrained by the maximal temperature allowed in the high-pressure steam turbine inlet (565°C).

The optimal oxygen purity (y_{O2}) is 97mol% for the E-Matiant cycle and 90 mol% for the SCOC-CC cycle. The energy efficiency of the E-Matiant cycle increases up to an oxygen purity of 97 mol%, as increasing the oxygen purity reduces the power consumed by the CO_2 and O_2 compressors. However, after oxygen purity of 97 mol%, the power consumption of the air separation units becomes very high, and the cycle energy efficiency decreases. In the SCOC-CC, even with a greater power consumption of the CO_2 and O_2 compressors for lower oxygen purity, the mass flow rate in the gas turbine expander is higher, and consequently, the power produced by this expander. In this way, the optimal oxygen purity for the SCOC-CC is 90 mol%.

Table 7. Solution of the optimization problems.

	TIT (°C)	pr	HP (bar)	LP (bar)	CP (bar)	DT (°C)	y_{O2}	η_I (%)
SCOC-CC	1234	40	85	6.426	0.0774	28	0.9	49.14
E-Matiant	1350	34.91	-	-	-	28	0.97	47.65

The temperature, pressure, mass flow, unitary exergy cost, and composition of each stream of the SCOC-CC are presented in Tab. 8. Approximately 90% of the flue gases at the dehumidifier outlet (stream 12, Tab. 8) are recycled into the gas turbine compressor (stream 1, Tab. 8). The captured CO_2 (stream 15, Tab. 8) is composed of approximately 85mol% of CO_2. The streams with the highest unitary exergy cost are the streams after the condenser (stream 21, Tab. 8) and the dehumidifier (stream 12, Tab. 8), and the oxygen stream at the ASU outlet (stream 7, Tab. 8). The captured CO_2 stream (stream 21, Tab. 8) is composed of 79.34mol% of CO_2 because of the lower oxygen purity.

Table 8. SCOC-CC: Properties of each stream.

Stream	**T (°C)**	**p (bar)**	**m (kg/s)**	**k**	**y_{CO2} (mol %)**	**y_{H2O} (mol %)**	**y_{Ar} (mol %)**	**y_{N2} (mol %)**	**y_{O2} (mol %)**
1	32.0	1.01	38.83	15.78	79.34	3.73	6.60	10.33	0.00
2	432.9	40.50	38.83	1.83	79.34	3.73	6.60	10.33	0.00
3	1234.0	38.50	44.01	1.68	71.65	13.25	5.96	9.32	0.00
4	600.0	1.06	44.01	1.68	71.52	13.22	5.96	9.32	0.00
5	30.0	40.50	1.00	1.00	-	-	-	-	-
6	25.0	1.01	17.15	1.00	0.00	18.77	9.81	77.52	19.62
7	0.1	4.70	4.17	12.19	0.00	0.00	3.90	6.10	90.00
8	30.0	40.52	4.18	6.67	0.00	0.00	3.90	6.10	90.00
9	27.0	1.01	12.78	0.00	0.00	0.00	1.20	98.80	0.00
10	29.5	3.10	0.21	0.00	0.00	100.00	0.00	0.00	0.00
11	95.1	1.023	44.01	1.68	71.52	13.22	5.95	9.31	0.00
12	28.0	1.013	42.00	91.12	79.34	3.73	6.60	10.33	0.00
13	28.0	1.013	3.16	91.12	79.34	3.73	6.60	10.33	0.00
14	30.0	100.00	3.17	3.96	79.34	3.73	6.60	10.33	0.00
15	28.0	1.013	38.83	91.12	79.34	3.73	6.60	10.33	0.00
16	565.0	85.00	6.47	2.16	0.00	100.00	0.00	0.00	0.00
17	217.6	6.41	6.48	2.16	0.00	100.00	0.00	0.00	0.00
18	197.8	6.42	1.18	2.16	0.00	100.00	0.00	0.00	0.00
19	214.5	6.43	7.65	2.16	0.00	100.00	0.00	0.00	0.00
20	40.0	0.07	7.65	2.16	0.00	100.00	0.00	0.00	0.00
21	40.0	0.07	7.65	153.3	0.00	100.00	0.00	0.00	0.00
22	40.1	6.43	7.65	106.2	0.00	100.00	0.00	0.00	0.00
23	25.0	1.01	382.20	1.00	0.00	100.00	0.00	0.00	0.00
24	35.0	1.01	382.20	0.00	0.00	100.00	0.00	0.00	0.00
25	25.0	1.01	182.60	0.00	0.00	100.00	0.00	0.00	0.00
26	35.0	1.01	182.60	1.00	0.00	100.00	0.00	0.00	0.00
27	35.0	1.01	20.120	0.00	0.00	100.00	0.00	0.00	0.00

The temperature, pressure, mass flow, unitary exergy cost, and composition of each stream of the E-Matiant are presented in Tab.9. This Table shows that the temperature of the flue gases at the turbine outlet (stream 5, Tab.9) is approximately 100°C higher than the temperature at the gas turbine outlet of the SCOC-CC since there are no constraints related to the maximum temperature considered for steam turbines (565°C). The captured CO_2 (stream 15, Tab. 9) is composed of approximately 90.9% (mass) CO_2, as this cycle works with a higher optimal oxygen purity. The streams with the highest unitary exergy cost are the streams after the dehumidifier (stream 7, Tab. 9) and the oxygen stream at the ASU outlet (stream 13, Tab. 9).

Table 10. E-Matiant: Properties of each stream.

Stream	**T (°C)**	**p (bar)**	**m (kg/s)**	**k**	**y_{CO2} (mol %)**	**y_{H2O} (mol %)**	**y_{Ar} (mol %)**	**y_{N2} (mol %)**	**y_{O2} (mol %)**
1	678.3	36.75	43.50	2.15	90.8	3.8	5.4	0.00	0.00
2	30.0	36.75	3.89	7.47	0.0	0.0	3.0	0.00	97.0
3	30.0	36.75	1.00	1.00	-	-	-	-	-

4	1350.0	34.91	48.39	1.79	82.5	12.8	4.7	0.00	0.00
5	713.3	1.04	48.39	1.79	82.5	12.8	4.7	0.00	0.00
6	236.8	1.02	48.39	1.79	82.5	12.8	4.7	0.00	0,00
7	28.0	1.01	46.37	39.4	90.9	3.7	5.4	0.00	0.00
8	108.4	37.48	46.37	2.37	90.9	3.7	5.4	0.00	0.00
9	108.4	37.48	43.50	2.37	90.9	3.7	5.4	0.00	0.00
10	25.0	1.01	17.15	1.00	0.0	1.9	0.9	77.5	19.6
11	27.0	1.01	13.06	0.00	0.0	0.0	0.0	99.0	1.0
12	29.5	3.10	0.20	0.00	0.0	100.0	0.0	0.0	0.0
13	0.1	4.70	3.89	13.97	0.0	0.0	0.03	0.0	0.97
14	28.0	1.01	2.02	0	0.0	100.0	0.0	0.0	0.0
15	108.4	37.48	2.88	2.369	90.9	3.7	5.4	0.00	0.00
16	30.0	100.00	2.88	3.356	90.9	3.7	5.4	0.00	0.00
17	25.0	1.01	353.30	1	0.0	100.0	0.0	0.0	0.0
18	35.0	1.01	353.30	0	0.0	100.0	0.0	0.0	0.0
19	25.0	1.01	228.00	1	0.0	100.0	0.0	0.0	0.0
20	35.0	1.01	228.00	0	0.0	100.0	0.0	0.0	0.0

The heat removed from the cycles and the water consumption for cooling is shown in Tab. 10. It was considered that the cooling water enters the components at 25°C and leaves the components at 35°C. It is observed that the total cooling water consumption is higher in the SCOC-CC cycle. The O_2/CO_2 compressors water consumption is higher in the SCOC-CC because the pressure ratio of this compressors is higher than in the E-Matiant.

Table 10. Water consumption and heat removed.

	SCOC-CC		**E-Matiant**	
Component	**Heat removed (kW)**	**Water consumption (kg/s)**	**Heat removed (kW)**	**Water consumption (kg/s)**
Dehumidifier	7640.0	182.6	14780.0	353.3
Condenser (Steam cycle)	15986.0	382.2	-	-
4-stage CO_2 compressor	-	-	9539.0	228.0
O_2 compressor	840.3	20.1	735.5	17.58
CO_2 compressor	1844.0	44.1	820.7	19.62
Total	26292.0	630.0	25875.2	618.5

The power consumption of the components of each cycle is presented in Tab 11. The net power of SCOC-CC is 3% higher than E-Matiant net power. It is observed that the ASU power consumption is higher in the E-Matiant due to the higher oxygen purity utilized in this cycle. On the other hand, the O_2 compressor power consumption is higher in the SCOC-CC because with a lower oxygen purity, the oxygen stream produced by the ASU contains more impurities, which increases the O_2 compressor power consumption. The CO_2 compressor power consumption is higher in the SCOC-CC because of the lower oxygen purity. In the E-Matiant, the CO_2 stream is pre-compressed in the 4-stages intercooled compressor, which reduces the CO_2 compressor power consumption in comparison with the SCOC-CC CO_2 compressor.

Table 11. Components power production and consumption.

SCOC-CC	**Power (kW)**	**E-Matiant**	**Power (kW)**
Gas turbine		**Expander**	
Gas turbine compressor	-15533	Turbine	40188
Gas turbine expander	36005	**Compressor**	
Gas turbine net power	20164	4-stages intercooled compressor	-12830
Steam cycle		**-**	
High-pressure steam turbine	4247	-	
Low-pressure steam turbine	4697	-	
High-pressure water pump	-73,72	-	
Low-pressure water pump	-6,54	-	
Steam cycle net power	8864	-	
CO_2 and O_2 systems		**CO_2 and O_2 systems**	
CO_2 compressor	-1782,0	CO_2 compressor	-580,8
O_2 compressor	-952,6	O_2 compressor	-839,9

Air separation unit (ASU)	-3129,0	Air separation unit (ASU)	-3474,0
Total power CO_2 and O_2 systems	-5863,6	**Total power CO_2 and O_2 systems**	-5167,7
SCOC-CC net power	**23165**	**E-Matiant net power**	**22463**

Figure 3 shows the contribution of each component to the global irreversibility of the SCOC-CC. The components of the SCOC-CC that present the highest irreversibility are the combustion chamber, HRSG, and ASU. Furthermore, the components required for oxy-fuel combustion (ASU, dehumidifier, O_2 and CO_2 compressors) correspond to 14% of the total exergy destroyed in the SCOC-CC. The second law efficiency of the SCOC-CC is 49.64%. Figure 4 shows each component's contribution to the E-Matiant cycle's global irreversibility. The major contributors to the destruction of exergy in the E-Matiant cycle are the combustion chamber, ASU, 4-stages intercooled compressor and recuperator. The dehumidifier, ASU, and the O_2 and CO_2 compressors correspond to 23.9% of the total exergy destroyed. The second law efficiency of the E-Matiant cycle is 53.79%.

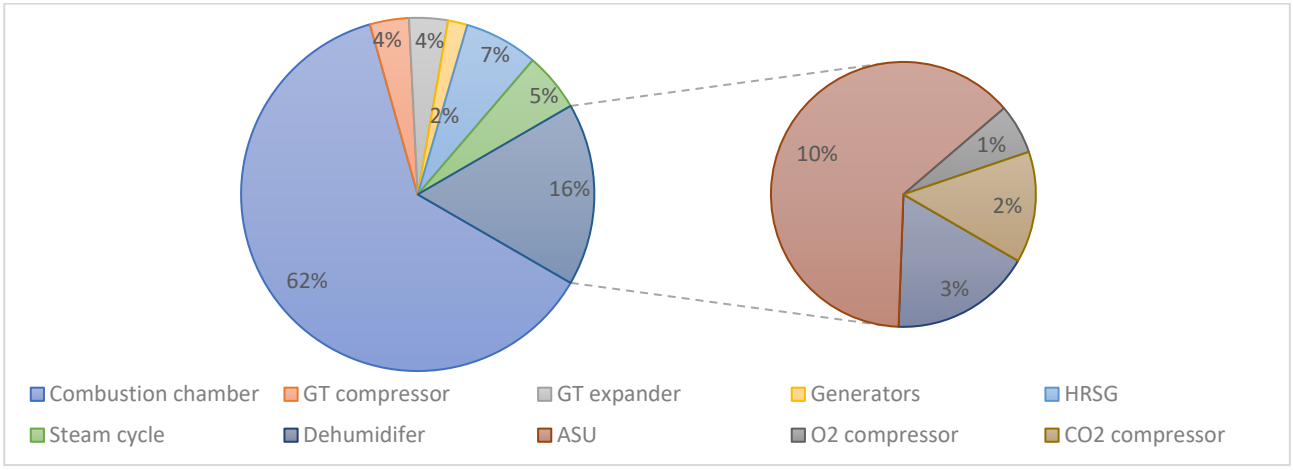

Figure 3. Semi-closed oxy-fuel combined cycle irreversibilities.

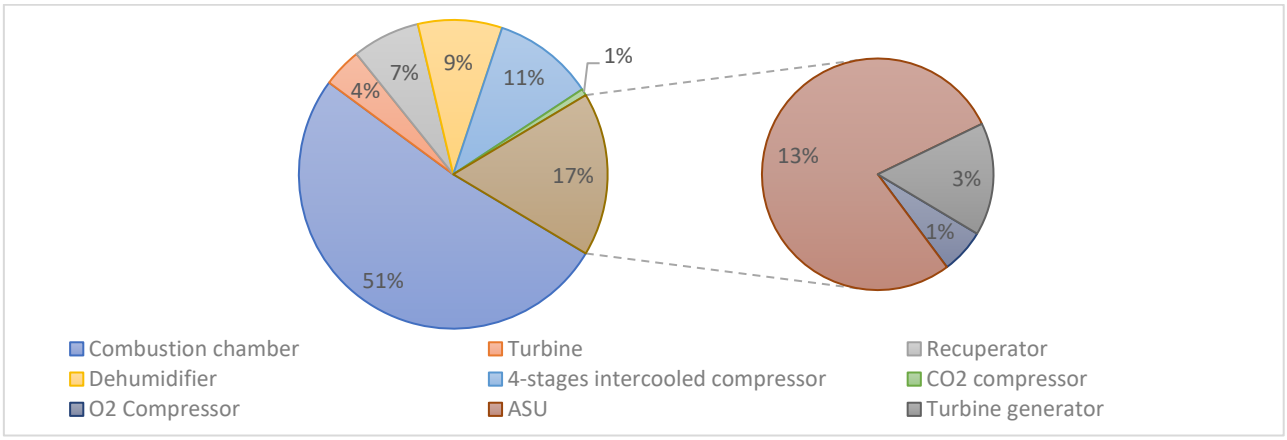

Figure 4. E-Matiant irreversibilities.

Table 12 shows the unitary exergy cost of the power produced in each cycle. It is observed that the unitary exergy cost of the net power of the E-Matiant is lower than that of the SCOC-CC, as the E-Matiant has a higher second law efficiency and less irreversibilities.

Table 12. Unitary exergy cost of the power produced.

SCOC-CC	**k**	**E-Matiant**	**k**
Gas turbine	1.772	Turbine	1.820
High-pressure steam turbine	2.281	-	-
Low-pressure steam turbine	2.481	-	-
Net power	1.945	Net power	1.848

4. CONCLUSIONS

In this work, E-Matiant and SCOC-CC cycles were analyzed. The energy efficiency of the SCOC-CC (49.14%) is higher than the E-Matiant (47.64%). The exergy efficiency of the E-Matiant (53.79%) cycle is higher than the SCOC-CC (49.64%), even having lower energy efficiency than the SCOC-CC. As the E-Matiant involves fewer components, fewer processes generate irreversibilities in the cycle. The E-Matiant cycle also has lower consumption of cooling water. Each of these cycles has its advantages and disadvantages, and both are good proposals to replace conventional gas plants, given that these cycles capture the CO_2 produced in the combustion process.

Some aspects of these cycles have to be further investigated. Future investigations highlight the importance of feasibility analysis of the cycles presented in this work. Investigating the potential usage or storage methods of the captured CO_2 is also essential.

5. REFERENCES

Bolland O., Thermal Power Generation, Department of Energy and Process Engineering - NTNU, 2010.

Dahlquist N. A., Conceptual Thermodynamic Cycle and Aerodynamic Gas Turbine Design-on an Oxy-fuel Combined Cycle. Lund, Sweden: Lund University; 2016.

Eberhart R. C., Kennedy J., Particle swarm optimization, Proceedings of the IEEE international conference on neural networks, Citeseer, 1995, Vol. 4.

Ebrahimi A. et al., Energetic, exergetic and economic assessment of oxygen production from two columns cryogenic air separation unit, *Energy 90*,2015, 1298-1316.

EPA. Overview of Greenhouse gases. Available at:<https://www.epa.gov/ghgemissions/overview-greenhouse-gases> [accessed 15.05.2022].

IEAGHG. Oxy-Combustion Turbine Power Plants. Report 2015/5; 2015.

GTW. Gas Turbine World: 2018 GTW Handbook (Vol. 33). Pequot Publishing, 2018.

Gülen S. C., Gas turbines for electric power generation. Cambridge University Press, 2019.

Hu Y., Li H., Yan J., Integration of evaporative gas turbine with oxy-fuel combustion for carbon dioxide capture, *International Journal of Green Energy*, 2010, *7*(6), 615-631.

Kehlhofer R. et al. Combined-cycle gas & steam turbine power plant., PennWell Books, LLC. 2009.

Kvamsdal H. M. Jordal K. Bolland O., A quantitative comparison of gas turbine cycles with CO2 capture, *Energy 2007*, v. 32, n. 1, p. 10-24.

Lozano, M. A., and A. Valero. "Theory of the exergetic cost." *Energy* 18.9 (1993): 939-960.

Metz B. et al., Carbon Dioxide Capture and Storage. *Special Report, Intergovernmental Panel on Climate Change*, Cambridge University Press; 2005.

Nascimento F.S., Simulação Numérica em CFD do Processo de Oxi-Combustão Aplicado ao Carvão Mineral Brasileiro para a Geração Termoelétrica. Itajubá, Brazil: Federal University of Itajubá; 2018.

National Energy Technology Laboratory (NETL). Commercial technologies for oxygen production – Available at:< https://www.netl.doe.gov/research/Coal/energy-systems/gasification/gasifipedia/commercial-oxygen> [accessed 15.05.2022].

Sheldrake A. L., Handbook of electrical engineering: for practitioners in the oil, gas and petrochemical industry. John Wiley & Sons, 2016.

Silva A. F., Lemonge A. C., S. L. Beatriz, Algoritmo de Otimização com Enxame de Partículas auxiliado por Metamodelos, In: XI Simpósio de Mecânica Computacional, II Encontro Mineiro de Modelagem Computacional, SIMMEC/EMMCOMP, Brazil, 2014.

Sundkvist S. G. et al., Concept for a combustion system in oxyfuel gas turbine combined cycles, *Journal of engineering for gas turbines and power 2014*, v. 136, n. 10.

United Nations. The Paris Agreement. Available at:<https://unfccc.int/process-and-meetings/the-paris-agreement/the-paris-agreement> [accessed 04.05.2022].

United Nations. Climate actions: Key findings – Available at:< https://www.un.org/en/climatechange/science/key-findings > [accessed 04.05.2022].

Zheng L. Oxy-fuel combustion for power generation and carbon dioxide (CO_2) capture. Elsevier, 2011.

6. RESPONSIBILITY NOTICE

The authors are the only responsible for the printed material included in this paper.